

## On the importance of soil damping for tall buildings loaded by wind

Gómez, S. S.; Geurts, C. P.W.; Metrikine, A.

**DOI**

[10.1016/j.engstruct.2017.11.029](https://doi.org/10.1016/j.engstruct.2017.11.029)

**Publication date**

2018

**Document Version**

Accepted author manuscript

**Published in**

Engineering Structures

**Citation (APA)**

Gómez, S. S., Geurts, C. P. W., & Metrikine, A. (2018). On the importance of soil damping for tall buildings loaded by wind. *Engineering Structures*, 163, 426-435. <https://doi.org/10.1016/j.engstruct.2017.11.029>

**Important note**

To cite this publication, please use the final published version (if applicable). Please check the document version above.

**Copyright**

Other than for strictly personal use, it is not permitted to download, forward or distribute the text or part of it, without the consent of the author(s) and/or copyright holder(s), unless the work is under an open content license such as Creative Commons.

**Takedown policy**

Please contact us and provide details if you believe this document breaches copyrights. We will remove access to the work immediately and investigate your claim.

# On the importance of soil damping for tall buildings loaded by wind

S.S. Gómez<sup>a,b,\*</sup>, C.P.W. Geurts<sup>b</sup>, A. Metrikine<sup>a</sup>

<sup>a</sup>*Faculty of civil engineering and Geosciences, Stevinweg 1, 2628CN Delft, The Netherlands*

<sup>b</sup>*TNO Structural dynamics, Van Mourik Broekmanweg 6, 2628XE Delft, The Netherlands*

---

## Abstract

In this paper, the overall damping as function of the velocity of vibration of two tall structures subjected to wind is studied. The overall damping ratio is studied by means of two simple, but representative and complementary models and it is compared with that identified in two buildings in The Netherlands. In the models, the soil-structure interaction is computed using the cone model for embedded foundations developed by Wolf. Relevant parameters of the structure are identified by means of experimental data and Jeary's damping predictor. The results of the modelling show a large contribution of the foundation damping ratio to the overall damping ratio when soft soil conditions are considered.

*Keywords:* Tall structure; damping; foundation damping; full-scale measurement;

---

## 1. Introduction

Tall buildings are designed according to the serviceability limit state SLS and the ultimate limit state ULS. The SLS is related to comfort levels and low vibration amplitudes commonly caused by wind gusts. On the contrary,  
5 the ULS is related to safety and high amplitude of vibration typically observed under earthquake scenarios.

---

\*Corresponding author

*Email addresses:* [sergio.sanchezgonzalez@tno.nl](mailto:sergio.sanchezgonzalez@tno.nl) (S.S. Gómez), [chris.geurts@tno.nl](mailto:chris.geurts@tno.nl) (C.P.W. Geurts), [A.Metrikine@tudelft.nl](mailto:A.Metrikine@tudelft.nl) (A. Metrikine)

*URL:* <http://www.elsevier.com> (A. Metrikine)

The earlier studies of dynamic behaviour of buildings were focused on ULS related to earthquake scenarios. Most of such studies were conducted by researchers in South California. One of the reasons to begin with this research was the devastating consequences of the San Francisco earthquake in February 1906. First fundamental results of the dynamic behaviour of a multistorey building under earthquake conditions were given by Blume [1] showing a general concurrence between computed and experimental fundamental periods. Furthermore, he established the basic assumption for the model implementation. Researchers from Japan [2] also attempted to formulate numerical models to understand and predict the dynamic behaviour of multistorey buildings. In 1960 Hudson [3], based on the work done by Blume, improved the numerical investigations of the building responses under earthquake scenarios. Funahashi and Kinoshita [4] investigated the consequences of a severe earthquake in Japan in 1923. In 1973 Hart [5] recorded the response of fourteen high-rise buildings in South-California during the San Fernando earthquake in 1971 and concluded that the modal damping increases approximately linearly with the amplitude at the fundamental period. Later, in 1975, Hart [6] pointed out that the work done in full-scale measurements was considerable [7-9]. In consequence, several approaches to identify the modal damping were developed. Furthermore, Hart introduced for the first time the concept of damping with respect to the amplitude of motion.

Nowadays, buildings are becoming taller but also lighter and more slender. Those characteristics make buildings more sensitive wind loads under SLS conditions. Damping is an important but most uncertain parameter in the dynamic response of buildings under wind excitations. The determination of the damping at the design stage of a building becomes crucial for the building performance. Davenport and Hill-Carrol [10] were the first to define intrinsic material damping, radiation damping, frictional damping and aerodynamic damping as the main mechanisms of energy dissipation in a tall building subjected to wind loads. They suggested a damping predictor based on full-scale measurements for the SLS of tall buildings. Jeary [11-12] also described the different mechanisms

of energy dissipation in a building and progressed further with the concept of amplitude dependent damping showing the relevance of the friction damping due to crack formation during high amplitude vibration and established a relation between damping and amplitude of vibration. Therefore, he proposed to distinguish three regimes of the total damping in buildings. These three regimes can be observed when a building structure vibrates near its fundamental frequency. The first regime is the low amplitude building vibration where damping behaves linearly with respect to the amplitude of the building vibration. In the second regime, the total damping increases non-linearly with the amplitude of the response of the building. The third regime represents the very high vibration amplitude more likely in earthquake situations. Therefore, each damping regime is named consequently: low amplitude plateau, non-linear regime and high amplitude plateau. Accordingly, he developed a damping predictor based on the full-scale measurements to determine the damping in the low amplitude plateau and the non-linear regime, since the high amplitude plateau was out of the scope of his work. Lagomarsino [13] claimed that the main mechanism of energy dissipation in steel buildings should be related to the friction in the joints, therefore the material damping is negligible. Consequently, he developed a theoretical model to predict friction damping in a building. However, he concluded that the model was not directly applicable and developed an empirical formula based on full-scale measurements. Tamura [14] formulated a damping predictor based on full-scale measurements for steel and concrete buildings and also went further implementing a friction model to describe the primary mechanism of damping during wind induced vibration [15, 16].

The relevance of the soil-foundation-structure interaction for the dynamic behaviour of a building has been pointed out [17-22]. The foundation damping can be related to the geometrical damping and the intrinsic damping in the soil. When a building vibrates, a soil-structure interaction process takes place (SSI). The soil involved in this interaction is very irregular. Therefore, the damping contribution of the soil due to the SSI is rather uncertain. This makes the soil-structure interaction effects a challenging subject matter to study. This

complexity was already pointed out by Jeary [12], who suggested that the soil-  
70 structure interaction is an uncertain process and becomes more predominant at  
the large amplitude of vibration due to the irregularity of the process. In 1956, a  
group of Japanese researchers [23-24] showed a summary of the results obtained  
from full scale measurements. They observed that during maximum ampli-  
tude of vibration of buildings, the contribution of swaying and rocking (motion)  
75 within the overall motion is strongly predominant. Besides, the rocking mo-  
tion becomes predominant as the stiffness of the structure increases relative  
to the stiffness of the ground. The conclusions about the foundation damping  
pointed out by the Japanese researchers and Jeary are based solely on observa-  
tions from full-scale measurements. Thus, there seems to be a lack of reliable  
80 modeling procedures to estimate the effect of SSI on the overall damping in the  
building.

Therefore, the aim of this paper is to close this gap within the framework of  
tall structures subjected to wind loads. In order to study the overall damping  
and the soil damping a discrete model and a continuous model representative  
85 for tall buildings are used. These models take into account the soil-structure  
coupling effects under small amplitudes of motion. Soil reaction to the horizontal  
and rocking motion of the building are modelled using the cone model developed  
by Wolf [25]. The energy dissipated in the structure is obtained using the linear  
component of Jeary's damping predictor. This is based on his statement in  
90 which he suggested the structural damping as the main mechanism of energy  
dissipation during low amplitude vibration. Based on literature [26], it can be  
stat that the first mode of vibration is the most predominant due to wind loads.  
Therefore, the parameters of the model are set to study the first building mode.  
Predictions of the mathematical models are compared to full-scale measurements  
95 on two tall buildings located in the Netherlands.

## 2. Problem description

In a building, there are many sources of energy dissipation, which are generally referred to as damping. The main issue to model damping in a building is that each source of energy dissipation can be governed by a different damping  
100 mechanism or by more than one damping mechanism activated in a different frequency or amplitude range.

The principal mechanisms of energy dissipation in the main load bearing structure (MLBS) are intrinsic material and friction damping, due to the crack development at large amplitudes. The non-structural elements (NSE) are also  
105 source of energy dissipation. The damping mechanism behind this group can be associated with the friction damping. However, it is reasonable to assume that this damping mechanism is activated when amplitudes of vibration are very large and initiate the non-linear behaviour. The aerodynamic damping is introduced to the structure by the wind. The aerodynamic damping has been  
110 extensively studied and models for that are available [27-28]. Furthermore, the joints or connections can be one of the main sources of energy dissipation due to friction between the connected surfaces of a building. The foundation, in one of its capacities radiates the energy of structural vibration into the soil, thereby serving as a source of the energy dissipation due to SSI. In this paper,  
115 the proposed sources of energy dissipation of a tall building are grouped and associated with the damping mechanisms described by Davenport and Hill-Carrol [10], as shown in Fig. 1.

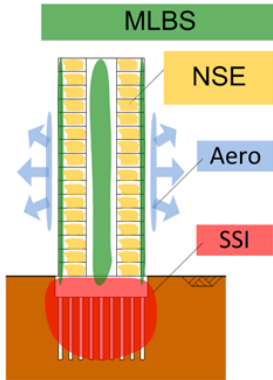


Figure 1: Damping sources in a high-rise building

### 3. Modelling approach

The damping of a tall structure with an embedded foundation is studied in this paper making use of a -three degree of freedom- model and a -continuous- model, see Figs. 2b and 3. This is done under the assumption of small amplitudes of vibration related to the SLS. Therefore, the friction damping caused by the NSE and other energy dissipation sources is assumed to be negligible. The aerodynamic damping is estimated based on the models presented in [27]. It can be shown that this damping mechanism has a negligible contribution to the total damping.

Given that, the procedure to compute the overall damping coefficient making use of an 3 DoF model is carried out as follows. First, the soil-structure interaction stiffness is parametrized by using the horizontal cone model  $K_{xx}$  and the rocking cone model  $K_{\theta\theta}$ . Next, the mass of the structure  $M_b$  is estimated based on [29]. Then, the structural stiffness  $K_b$  is tuned such that the fundamental frequency  $\omega_N$  matches the experimentally identified fundamental frequency.

Then  $C_{xx}$  and  $C_{\theta\theta}$  are computed based on Wolf's formulation [25]. Finally  $C_b$  which represents the structural and material damping in the MLBS and the NSE is computed by means of the Jeary's formulation (Eq.1). The overall damping ratio is obtained by means of analysis of the free vibration of the

structure. The motion of the structure is a result of interaction between the structure and the foundation in combination with the soil. Therefore, both the damping in the structure and in the foundation influence the overall behaviour  
140 of the system.

The discrete model contains visco-elastic elements (springs and dashpots) concentrated at specific locations. Therefore, relative deformations along the structure cannot be taken into account. This might lead to the underestimation of damping in the structure, specially at the bottom of the structure, where  
145 stresses are larger. In order to deal with this issue, a continuous model is used to complement the study carried out with the 3 DoF model. The characterization of the continuous model is accomplished by means of the uniformly distributed mass density  $\rho A$ , bending stiffness  $EI$  and material damping  $E^*$ . Further, both the 3 DoF model and the continuous model account for the mass moment of  
150 inertia  $I_b$ , height  $H$  and embedment  $h$ . The foundation is assumed to be rigid, of a rectangular shape and of negligible thickness and it is characterized by the mass  $M_0$  and mass moment of inertia  $I_0$ . The motion of the soil is coupled to that of the foundation. In the models,  $u(t)$  is the horizontal displacement of the building with respect to the ground,  $u_{xx}(t)$  is the horizontal displacement  
155 of the ground with respect to a fixed reference point, and  $\varphi_{\theta\theta}(t)$  represents the rocking angle of the ground.

In this paper, linear models are used, whose damping ratio is independent of the initial condition and of the amplitude of motion. However, results are presented in terms of decidedness of the damping on the initial velocity, in order  
160 to compare those with experimental data.

## 4. The models

### 4.1. A discrete model

The model sketched in Fig. 2a is adopted in this study. The stiffness and damping of the building and the soil can be represented by means of springs

165 and dashpots assuming small displacements. The viscous structural damping is modelled with the linear component of the Jeary's empirical damping predictor:

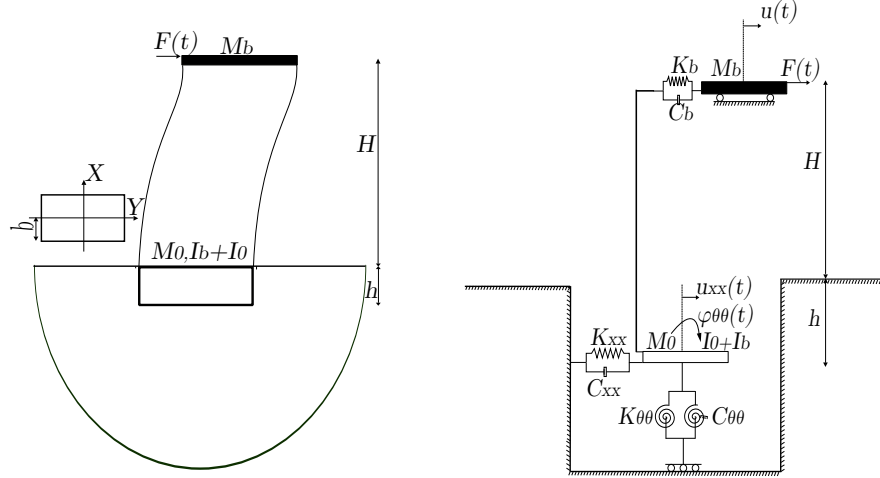
$$\xi_b = \left(0.15 + \frac{46}{H}\right) 0.01 = \frac{C_b}{2\sqrt{K_b M_b}} \quad (1)$$

where  $H$  represents the height of the building in meters.

It should be noted that the Jeary's damping predictor accounts for all sources of energy dissipation in a building including the SSI. The first term in Eq. 1 accounts for the structural damping while the second term ( $46/H$ ) is associated with the SSI effect in which damping decreases with the building height due to the fact the lower the frequency of structural vibration, the smaller the radiation and material damping provided by the SSI. Therefore, the assumption formalized by Eq. 1 that this predictor describes damping in the building only (excluding damping associated with SSI) must overestimate the energy dissipation in the building provided that the predictor is conservative. In this paper we will show, however, that additional damping due to soil-structure interaction is needed in order to reproduce measurements. This will clearly demonstrate that the contribution of SSI to the total damping is underestimated by Jeary's predictor, which, essentially, is one of the main goals of the paper. The stiffness and damping of the foundation are computed by horizontal and rotational springs and dashpots by means of the cone model derived by Wolf (Eqs. 19-20).

#### 4.1.1. Governing equations of the discrete model

The equations of motion of the system shown in Fig. 2b can be written as follows,



(a) Interpretation of a high-rise building

(b) Model of a high-rise building

Figure 2: Model of a high-rise building on rigid foundation that takes into account flexibility of the soil

where  $u_r(t) = u(t) - u_{xx}(t)$

$$M_b [\ddot{u}_r(t) + \ddot{u}_{xx}(t)] + \left( K_b + C_b \frac{\partial}{\partial t} \right) [u_r(t) - (H + h)\varphi_{\theta\theta}(t)] = F(t) \quad (2)$$

$$M_0 \ddot{u}_{xx}(t) + \left( K_b + C_b \frac{\partial}{\partial t} \right) [(H + h)\varphi_{\theta\theta}(t) - u_r(t)] + \left( K_{xx} + C_{xx} \frac{\partial}{\partial t} \right) u_{xx}(t) = 0 \quad (3)$$

$$(I_0 + I_b) \ddot{\varphi}_{\theta\theta}(t) + \left( K_{\theta\theta} + C_{\theta\theta} \frac{\partial}{\partial t} \right) \varphi_{\theta\theta}(t) + \left( K_b + C_b \frac{\partial}{\partial t} \right) [(H + h)\varphi_{\theta\theta}(t) - u_r(t)] (H + h) = 0 \quad (4)$$

Eq. (2) represents the horizontal force equilibrium of the structure, Eq. (3) represents the horizontal force equilibrium of the soil-foundation interaction and

Eq. (4) represents the moment equilibrium of the soil-foundation interaction of  
 190 the system. The system of equations Eqs. (2)-(4) can be rewritten in the  
 following matrix form,

$$\mathbf{M}\ddot{U}(t) + \mathbf{C}\dot{U}(t) + \mathbf{K}U(t) = F(t) \quad (5)$$

$$[\mathbf{M}] = \begin{bmatrix} M_b & 0 & 0 \\ 0 & M_0 & 0 \\ 0 & 0 & I_0 + I_b \end{bmatrix} \quad (6)$$

$$[\mathbf{K}] = \begin{bmatrix} K_b & -K_b & -K_b(H+h) \\ -K_b & K_b + K_{xx} & K_b(H+h) \\ -K_b(H+h) & K_b(H+h) & K_b + K_{\theta\theta}(H+h)^2 \end{bmatrix} \quad (7)$$

$$[\mathbf{C}] = \begin{bmatrix} C_b & -C_b & -C_b(H+h) \\ -C_b & C_b + C_{xx} & C_b(H+h) \\ -C_b(H+h) & C_b(H+h) & C_b + C_{\theta\theta}(H+h)^2 \end{bmatrix} \quad (8)$$

$$F(t) = \begin{bmatrix} f(t) \\ 0 \\ 0 \end{bmatrix} \quad (9)$$

$$U(t) = \begin{bmatrix} u(t) \\ u_{xx}(t) \\ \varphi_{\theta\theta}(t) \end{bmatrix} \quad \dot{U}(t) = \begin{bmatrix} \dot{u}(t) \\ \dot{u}_{xx}(t) \\ \dot{\varphi}_{\theta\theta}(t) \end{bmatrix} \quad \ddot{U}(t) = \begin{bmatrix} \ddot{u}(t) \\ \ddot{u}_{xx}(t) \\ \ddot{\varphi}_{\theta\theta}(t) \end{bmatrix} \quad (10)$$

and subsequently cast in the state-space form. Now, Eq. (5) can be trans-  
 formed to the frequency domain as follows,

$$\mathbf{A}(\omega)\tilde{U}(\omega) = F(\omega) \quad (11)$$

195 where  $\mathbf{A}$  is a matrix that contains the mass, damping and stiffness coeffi-  
 cients. Setting the determinant of  $\mathbf{A}$  to zero and solving for the roots of the  
 obtained equation, complex valued natural frequencies can be found.

The experimental results are presented in the time domain therefore, for consistency, the system of equations cast in the matrix form are also solved in  
 200 the time domain as follows,

$$\dot{U}(t) = V(t) \tag{12}$$

$$\dot{V}(t) = \mathbf{M}^{-1}F(t) - \mathbf{M}^{-1}\mathbf{C}V(t) - \mathbf{M}^{-1}\mathbf{K}U(t) \tag{13}$$

In order to analyze the system dynamics in the time domain the Euler integration scheme was used.

#### 4.2. A continuous model

Figure 3 shows a tall structure modelled as an Euler-Bernoulli beam, in  
 205 which the mass per unit length  $\rho A$ , material damping  $E^*$ , structural damping  $C_b$  and bending stiffness  $EI$  are uniformly distributed along the beam. The foundation is accounted for as boundary conditions at the lower end of the beam as shown in Eq. (15).

##### 4.2.1. Governing equations of the continuous model

210 The equation of motion and the boundary conditions of the system sketched in Fig. 3 can be written as follows,

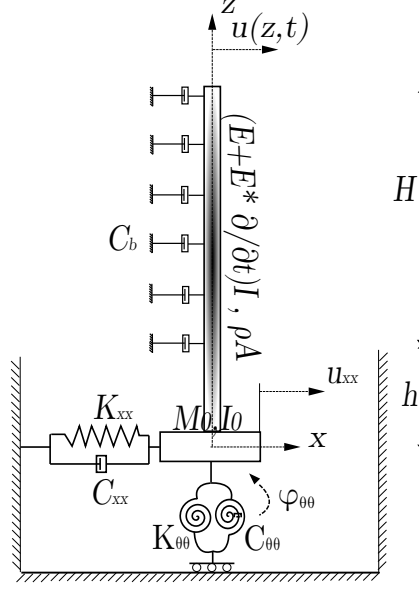


Figure 3: Model of a high-rise building with a Continuous beam

$$\rho A \frac{\partial^2 u(z,t)}{\partial t^2} + C_b \frac{\partial u(z,t)}{\partial t} + \left( E + E^* \frac{\partial}{\partial t} \right) I \frac{\partial^4 u(z,t)}{\partial z^4} = F(t) \quad (14)$$

for,  $z = 0$

$$\begin{aligned} \left( E + E^* \frac{\partial}{\partial t} \right) \frac{\partial^2 u(0,t)}{\partial z^2} &= K_{\theta\theta} \varphi_{\theta\theta}(0,t) + C_{\theta\theta} \frac{\partial \varphi_{\theta\theta}(0,t)}{\partial t} + I_0 \frac{\partial^2 \varphi_{\theta\theta}(0,t)}{\partial t^2} \\ - \left( E + E^* \frac{\partial}{\partial t} \right) I \frac{\partial^3 u(0,t)}{\partial z^3} &= K_{xx} u_{xx}(0,t) + C_{xx} \frac{\partial u_{xx}(0,t)}{\partial t} + M_0 \frac{\partial^2 u_{xx}(0,t)}{\partial t^2} \end{aligned} \quad (15)$$

for,  $z = H + h$

$$\left( E + E^* \frac{\partial}{\partial t} \right) I \frac{\partial^2 u(L,t)}{\partial z^2} = \left( E + E^* \frac{\partial}{\partial t} \right) I \frac{\partial^3 u(L,t)}{\partial z^3} = 0 \quad (16)$$

and the kinematic relations

$$u(0,t) = u_{xx}(t) \quad (17)$$

$$\frac{\partial u}{\partial z}(0,t) = \varphi_{\theta\theta}(t) \quad (18)$$

Where,  $E^* \frac{\partial}{\partial t}$  is the Kelvin-Voigt viscous damping model and represents the internal material damping. By using this model, the energy dissipation due to the stresses in the material can be taken into account. In order to account for damping associated with small relative motion of structural elements, a viscous damping is introduced that is characterized by a distributed layer of linear viscous elements  $C_b$ .

Due to the presence of damping operators in the boundary conditions Eqs. (15) and (16), the classical method of separation of variables cannot be applied. Therefore, the equations of motion and boundary conditions are transformed to the Fourier domain.

The transformed equation of motion Eq. (14) and the boundary conditions Eqs. (15) and (16) can be used to obtain the frequency equation Eq. (19), whose complex-valued roots are the natural frequencies of the system.

$$\det \mathbf{A}(\beta_i) = 0 \quad (19)$$

In Eq. (19)  $\mathbf{A}$  is a 4x4 matrix containing the boundary equations, where  $\beta_i$  is defined as,  $\beta_i^4 = \frac{\rho A \omega^2 - i \omega C_b}{EI + E^* i \omega}$ .

#### 4.3. Foundation model

In order to model the foundation, the cone model for embedded foundations developed by Wolf [25] is used.

$$K_{xx} = 2 \frac{\rho c_s^2}{z_{0,h}} \pi r_{0,h}^2 \quad (20)$$

and

$$K_{\theta\theta} = 2 \frac{3 \rho c_s^2}{z_{0,\theta}} \frac{\pi r_{0,\theta}}{4} \quad (21)$$

with,

$$\frac{z_{0,h}}{r_{0,h}} = \frac{\pi}{32} \frac{7-8\nu}{1-\nu} \quad \frac{z_{0,\theta}}{r_{0,\theta}} = \frac{9\pi}{128} \frac{3-4\nu}{1-\nu} \frac{c^2}{c_s^2} \quad (22)$$

Where,  $\rho$  is the soil density,  $c_s$  and  $c$  are the shear and pressure wave speed respectively,  $r_{0,h}$  and  $r_{0,\theta}$  are the equivalent ratios of the foundation size. The Wolf model is based on elastic theory and takes the assumption that a rigid disk resting of a half-space loaded by a dynamic load produces a wave propagation, that can be represented by a cone. This cone is described by the opening angle with respect to the equivalent foundation radius  $\frac{z_{0,h}}{r_{0,h}}$ ,  $\frac{z_{0,\theta}}{r_{0,\theta}}$ . Assuming that, the disks are much stiffer than the soil around, the foundation embedment can be represented by a stack of disks stick together and the wave pattern can be physically represented by a double-cone, which described waves going upwards and downwards.

## 5. Measurements of wind-induced vibrations

### 5.1. Building description and instrumentation

#### 5.1.1. The Churchill tower

The Churchill tower is a 70m office building with 24 storeys. The building was built in the early 70's and renovated thirty years later. The Churchill tower is a concrete building with a rectangular shape as well as its foundation. The horizontal stability of the building is achieved by the main core. The floors span from the main core to the external columns.

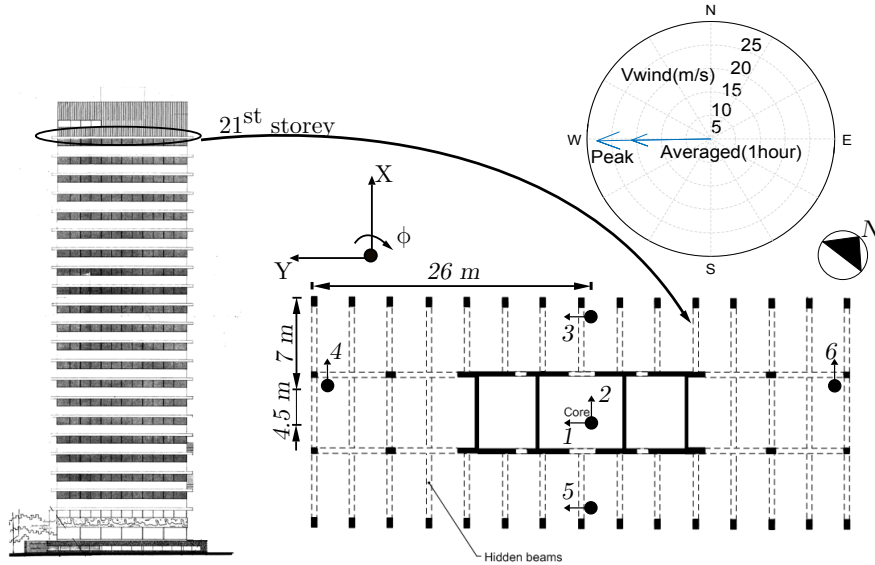


Figure 4: Churchill Tower layout

The vertical loads on the floors are transferred to the hidden beams shown  
 255 in Fig. 4. The beams transfer the loads to the columns and the core. These  
 elements transfer the loads directly to the foundation. The building is erected  
 on a soft soil environment.

The building has been instrumented with 6 Sundstrand accelerometers at  
 the highest possible location of the tower (storey 21<sup>th</sup>), as shown in Fig. 4.  
 260 Accelerometers 1, 3 and 5 are placed along the long horizontal dimension mea-  
 suring in the strong direction. Accelerometers 2, 4 and 6 are located along the  
 short horizontal dimension measuring in the weak direction. During the mea-  
 surements, the wind was blowing in the west direction. This instrumentation  
 strategy is followed in order to capture the fundamental modes of the building.

#### 265 5.1.2. The Erasmus Medical Center (E.M.C)

The New Erasmus Medical Center is a building of 121,5m height. The build-  
 ing has a uniform rectangular shape. The horizontal stability of the building is  
 accomplished by means of a concrete core and a tube as shown in Fig. 5. The

lower part of the concrete core is made in-situ, while the larger part of the core,  
 270 tube and floors are made out of prefabricated concrete.

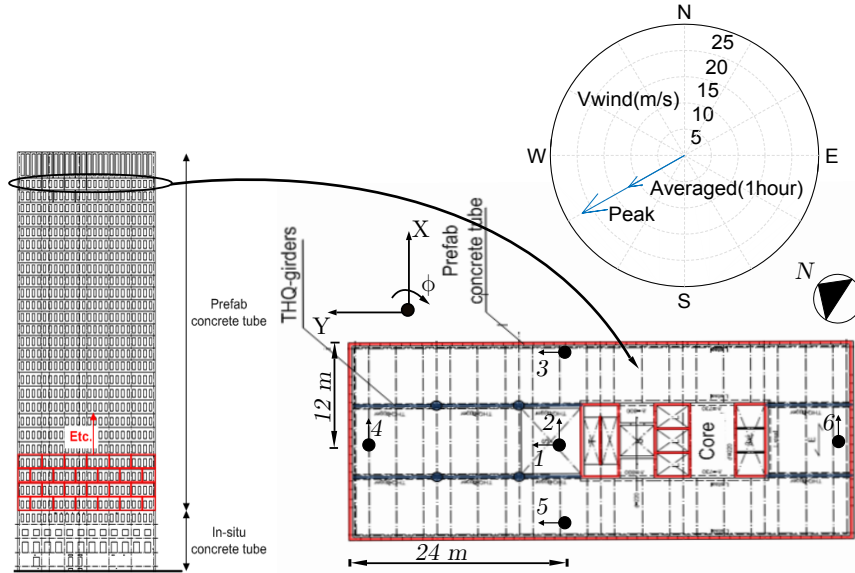


Figure 5: E.M.C layout

The floors are connected to the core and the tube. The wind-induced loads are transferred to the foundation through the tube principally, but also from the core. The location of the building contains a very soft soil conditions with a large clay layer.

275 In this case, the instrumentation strategy is similar to the previous case study. The building has been instrumented with 6 Sundstrand accelerometers at the top floor as shown in Fig. 5. This instrumentation set up is very convenient for rectangular shape structures. Three accelerometers (1, 2 and 3) are placed along the long horizontal dimension measuring in the strong direction  
 280 and, another three accelerometers (4, 5 and 6) are located along the short horizontal dimension measuring in the weak direction. During the measurements, the wind was blowing in the south-west direction.

## 5.2. Field measurements

Acceleration measurements were carried out in both buildings under strong  
285 wind conditions, as shown in Figs. 4-5. Accelerations were recorded during  
two hours for the two study cases. The Churchill tower was instrumented and  
measured on 25-11-2005 between 10:00 - 12:00h am. Measurements on the New  
Erasmus Medical center were performed on 6-9-2011 from 18:00 to 20:00h pm.  
Detailed specifications of the instrumentation are summarized in Table 1.

	Sensors	Characteristics
The churchill tower	Accelerometers	Filtering 5Hz Sampling frequency 100 Hz Calibration range $19.62V/m/s^2$ Voutput=9.81 V
The E.M.C	Accelerometers	Filtering 5Hz Sampling frequency 50 Hz Calibration range $19.62V/m/s^2$ Voutput=9.81 V

Table 1: Instrumentation description

290 Acceleration data were recorded and stored in sub-samples of 10 minutes.  
After some data processing, time traces of each sensor were transformed into  
the frequency domain for identification.

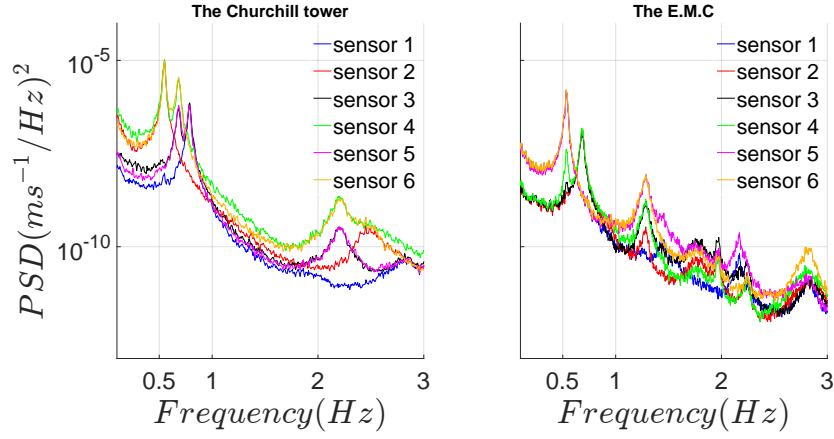


Figure 6: Power spectral density function of the instrumented buildings

Measurements show in both case studies a coupled behaviour of the translational and rotational motions. Therefore, modal analysis techniques based on a single degree of freedom (SDoF) cannot be applied. In order to deal with this issue, the accelerometers signatures have been rotated and the recorded acceleration signals have been numerically integrated and recombined by means of rigid body kinematics.

$$\vec{v}_B = \vec{v}_A + \vec{\omega} \times \vec{r}_A^B \quad (23)$$

Equation 23 implies that the velocity at  $B$  can be computed as the velocity at  $A$  plus the angular velocity  $\omega$  times the distance from  $A$  to  $B$ . This leads to the results shown in Fig. 7:

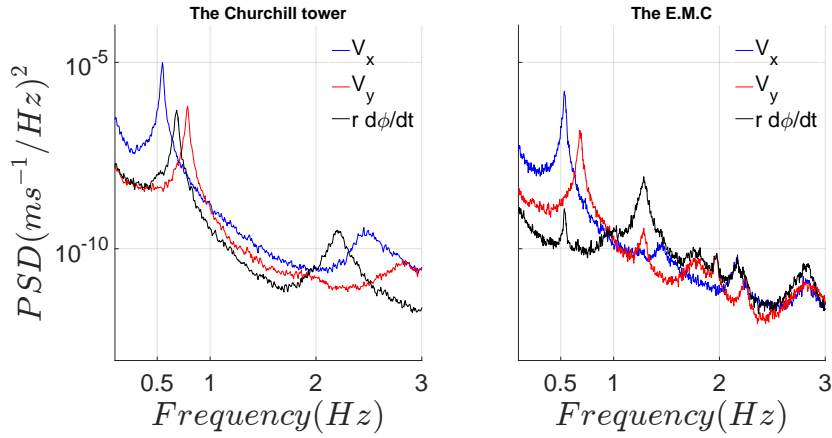


Figure 7: Power spectral density function of the instrumented buildings

Having separated the signals to a singular mode SDoF, standard identification techniques can be applied. In this study, the the half-power bandwidth technique (HPBW) is adopted in order to identify the fundamental frequency and equivalent viscous damping value.

305

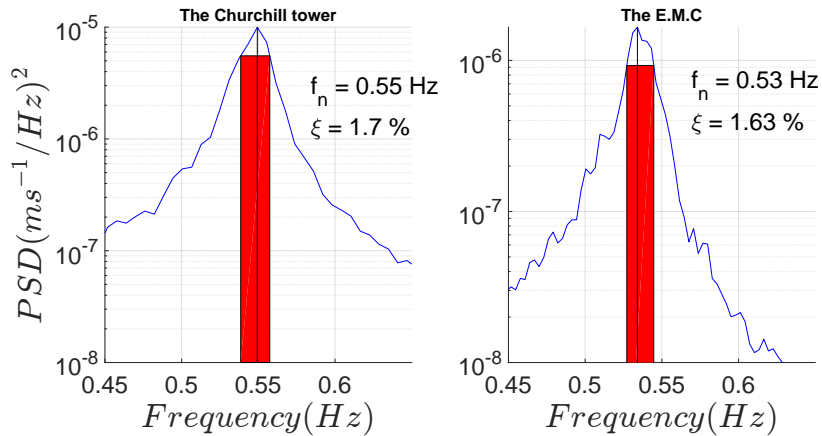


Figure 8: Power spectral density function of the instrumented buildings

The fundamental frequency in each direction can be straightforwardly identified by matching the spikes of the spectrum with the horizontal axis (frequency

axis). The overall damping is identified by means of the frequency response function of an SDoF system when the ratio between the fundamental frequency and the excitation frequency is close to one. Then, the following expression can be used to obtain a damping ratio.

$$2\xi = \frac{\Delta f}{f_0} \quad (24)$$

Where  $f_0$  is the frequency value of the fundamental frequency and  $\Delta f$  is the frequency span at square root of two of the peak height.

## 6. Results

The models presented in section 4 are used to study the overall damping behaviour of the structural system and the influence of the foundation damping on the overall damping experienced by the building in the regime of small vibrations. The outcome of the model is compared with experimental data gathered from 2 instrumented buildings in the Netherlands presented in section 5. In this study, the first fundamental mode of the buildings is targeted and the measured results are compared with predictions of the models. This is done because measurements show that vibrations in the weak direction are dominant leading to larger accelerations (Fig. 7) compared to the other directions. Due to the lack of experimental data regarding the soil stiffness at locations of the buildings, theoretical values corresponding to soft soils characteristics of the locations of the buildings were used. Besides, a sensitivity analysis as to the effect of the soil stiffness is conducted. The soil shear wave speed  $V_{s_{soil}}$  ranging between 100m/s to 130m/s in the case of soft soil study, and from 130 m/s to 266 m/s in the case of stiff soil study, soil density of  $\rho = 1900\text{Kg/m}^3$  and Poisson ratio of  $\nu = 0.3$  are chosen as the soil characteristics. The mass moments of inertia are expressed as  $I_b = \frac{1}{3}M_b b^2$  and  $I_0 = \frac{1}{3}M_0 b^2$ . The geometry, the natural frequency and the damping ratio of the first mode of the buildings are summarized in Table 2. The natural frequency  $\omega_n$  and the overall damping ratio  $\xi$  were identified from the measurements by means of the half-power bandwidth method (HPBW).

	Dimensions[m]	Storeys	$\omega_n$ [rad/s]	$\xi$ [%]	Max. disp.top [m]
The Churchill tower	Height 70 Width 52 Depth 23	24	3.45	1.7	$2.1e^{-3}$
The E.M.C	Height 121.5 Width 48 Depth 24	31	3.35	1.63	$0.6e^{-3}$

Table 2: Buildings characteristics

335
340
345
350
In order to determine equivalent stiffness of the studied buildings to parametrize the models presented in section 4, the experimental data is used. Due to the significant influence of the soil-building interaction, the stiffness needs to be identified indirectly. This is done using the three degree of freedom model given by Eqs. (2)-(4). First, the horizontal  $K_{xx}$  and rotational  $K_{\theta\theta}$  soil stiffness are computed by means of Eqs. (20) and (21) for the range of  $V_{s_{soil}}$  described above. Second, the natural frequency ( $w_n = 2\pi f_n$ ) of the building is identified. Having an estimation for the building mass  $M_b$  and foundation mass  $M_0$ , and setting all damping terms to zero,  $K_b$  is the only parameter that remains unknown in Eqs. (2)-(4). This can be done due to the fact that damping associated to building structures is low and affects marginally the fundamental frequency. Then,  $K_b$  is tuned such that the resultant fundamental frequency of the model by applying the eigenvalue problem is matched to the identified fundamental natural frequency of the building. By doing so, the best fit for the building stiffness  $K_b$  as function of the shear wave speed  $V_{s_{soil}}$  within the defined range is found. Figure 9, shows the identified  $K_b$  versus the  $V_{s_{soil}}$ .

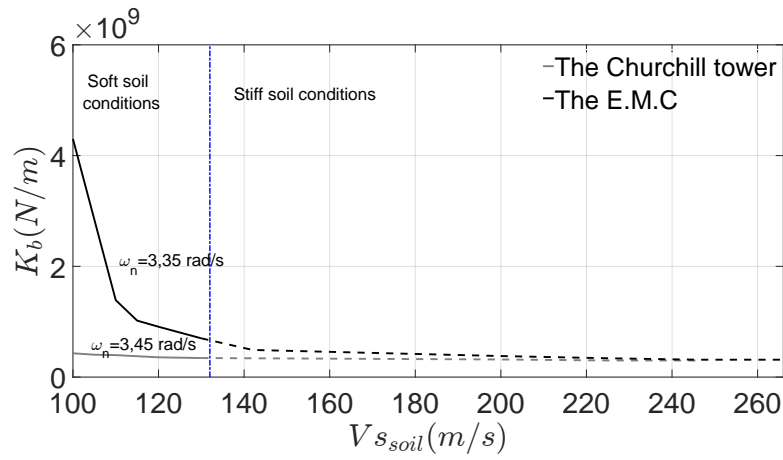


Figure 9: Stiffness of the building as function of soil shear wave speed

In the case of the E.M.C, the building stiffness  $K_b$  is highly dependent on the soil stiffness. This suggests that the soil conditions where the E.M.C is located are extremely soft. Therefore, higher building stiffness is required in order to match the identified natural frequency.

355 *6.1. Study of damping*

In this section, damping is studied and compared to full-scale measurements. In order to obtain equivalent viscous damping with respect to the velocity of the building at the measured locations the random decrement technique (RDT) [30] was applied to the experimental data. The procedure to obtain damping  
 360 with respect to velocity from the acceleration signals is described in Fig. 10.

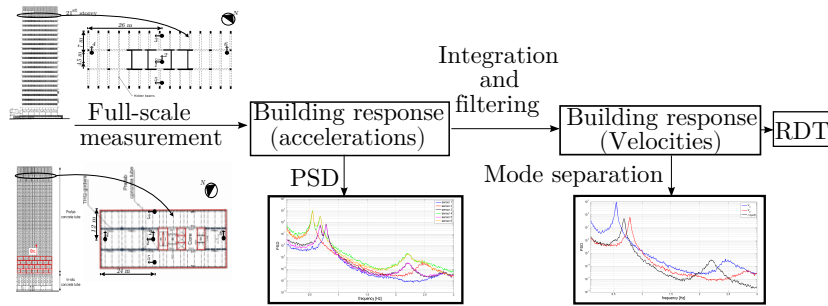


Figure 10: Description of the application of the RDT

The RDT enables us to transform stochastic signals as the measured in buildings due to wind loads into exponentially decaying signals by minimizing the random effects coming from the load. Therefore, after applying the RDT, SDoF identification techniques such as the exponential logarithmic decay can be applied to assess equivalent viscous damping. This procedure is reproduced for several velocity levels of the measured signal leading to a figure where damping is plotted versus the velocity of the building at the measured location. However, for the correct assessment of damping by means of the RDT, a large amount of averages over the specific velocity level are needed, which most of the times makes the assessment not feasible at peak velocities due to lack of high velocity peaks within the measurement period. Given that, high velocity levels are left out in the results shown in Figs. 11-13. In order to compare experimental damping results with modelling results, the initial velocity of each exponential decay obtained by applying the RDT to the experimental data is used as initial condition for the models letting the model vibrate freely reproducing the exponential decays obtained experimentally.

### 6.1.1. The Churchill tower

The information extracted from the measurements shows an amplitude-independent behaviour of the damping ratio. This observation justifies our choice to relate the damping coefficient  $C_b$  to the linear component of Jeary's formula.

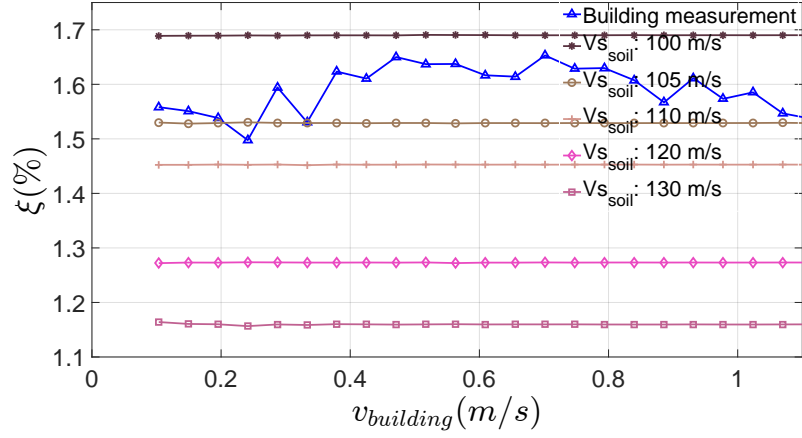


Figure 11: Damping ratio with respect to the velocity from the measurement of the Churchill tower and the discrete model

Fig. 11 shows the overall equivalent viscous damping within a building velocity range. The velocity  $v_{building}$  corresponds to the mean velocity of 10 minutes time records at the locations where measurements were performed by applying the RDT. The damping ratio predicted by the model is equivalent to the damping identified from the experimental data within the range of  $V_{s_{soil}} = 105 - 130$  m/s. Further, a clear dependence of the overall damping on the soil stiffness can be clearly seen in Fig. 11. The contribution of the foundation damping to the overall damping can be studied making use of Fig. 12, which shows the relative contribution of the foundation damping as function of the soil stiffness.

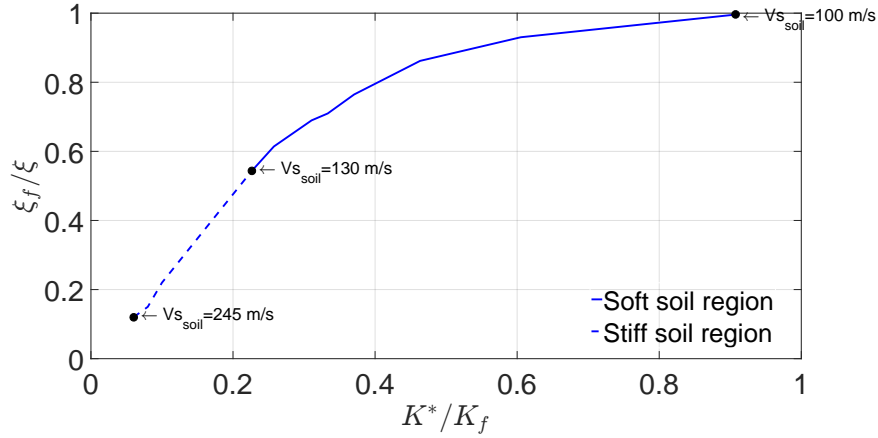


Figure 12: Foundation damping influence with respect to the stiffness in the Churchill tower

The total stiffness of the system  $K^*$  used to plot Fig. 12 is calculated as follows,

$$\frac{1}{K^*} = \frac{1}{K_b} + \frac{1}{K_f} \quad (25)$$

where,

$$\frac{1}{K_f} = \frac{1}{K_{xx}} + \frac{(H+h)^2}{K_{\theta\theta}} \quad (26)$$

395 The overall damping  $\xi$ , which contains  $C_{xx}$  and  $C_{\theta\theta}$  computed by means of the Wolf model and  $C_b$  computed by means of the Jeary's formula is assessed by running the simulations of the model at each specific velocity level and identifying the damping from the exponential decay. The foundation damping  $\xi_f$  is calculated by means of the same procedure, but setting  $C_b$  to zero.

400 Fig. 12 clearly shows the foundation contributes more than 60% to the overall damping in case of soft soil characteristics, which is a very substantial contribution that must be accounted for in design. The contribution of the foundation damping as obtained above can be subject to discussion due to

the fact that the material and structural damping  $C_b$  are concentrated in a  
405 single degree of freedom in the employed model, while in reality it is distributed  
along the structure. In order to check whether the continuous distribution of  
damping in the building will effect our conclusion as to the significant effect of  
the foundation damping, the continuous beam model described in the previous  
section is studied for the case of  $V_{s_{soil}} = 105$  m/s. This is done in the following  
410 manner. The foundation model is kept unchanged with respect to the one  
used in the 3DoF model. Then, the distributed damping is tuned such as to  
give the same total fundamental complex-valued frequency. After matching the  
overall damping with that obtained with the discrete model, the damping in the  
building in the continuous model was increased by about 60% with respect to  
415 that used in the discrete model. This led to an increase of 15% in the overall  
damping, which allows us to conclude that the effect of the foundation damping  
is dominant and is not significantly influenced by the choice of the model for  
the building.

### 6.1.2. *The E.M.C*

420 Fig. 13 shows a comparison between the velocity-independent damping ratio  
obtained from the experimental data and predictions of the discrete model.

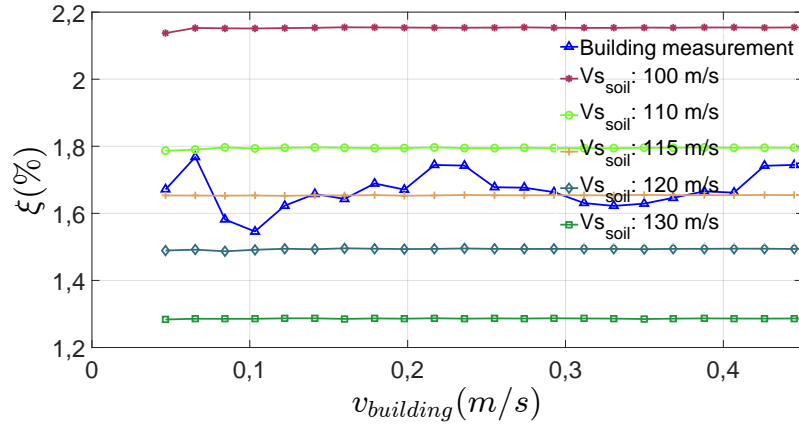


Figure 13: Damping ratio as a function of the velocity from the measurement of the E.M.C tower and the predictions of the discrete model

In this case the damping ratio predicted by the model is equal to the damping obtained from the experimental data when the  $V_{s_{soil}} = 115$  m/s.

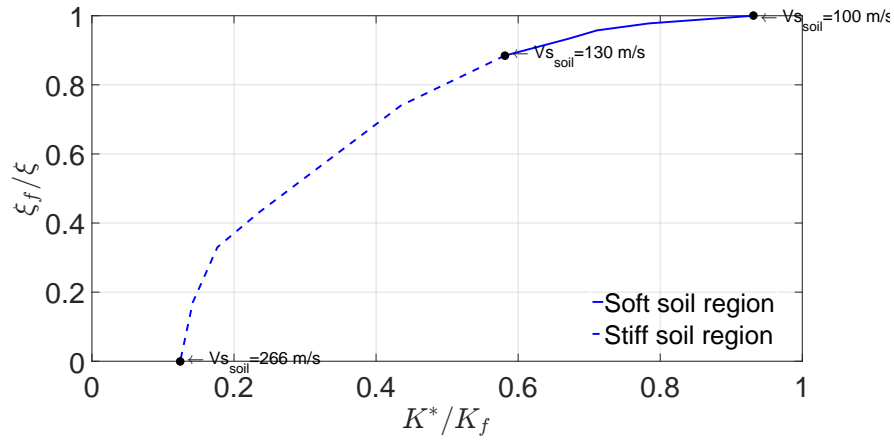


Figure 14: Foundation damping influence with respect to the stiffness in the E.M.C tower

Fig. 14 shows that the contribution of the foundation damping for this building is even higher than for previous one in the case of soft soil conditions. Now, as in the previous case, the continuum model will also predict a significant

contribution of the foundation damping. Increase of the damping in the building by 60% led to a marginal increase of 9% in the overall damping. This confirms the model-independent significance of the foundation damping.

## 430 7. Conclusions

It has been shown in this paper, that dissipation of energy at the soil-structure interface plays an important role in wind-induced vibrations of high-rise buildings. Two basic models have been considered in the paper, both accounting for the structural and soil damping. First model is a 3 degrees-of-  
435 freedom lumped parameter model, which takes into account the first translational mode of the building and the rotation and lateral translation of the foundation. Second model adopts a bending beam to describe the building, whereas the foundation is accounted for in the boundary conditions. Parameters of the models have been tuned to correspond with results of full-scale measurements  
440 performed at two buildings located in The Netherlands. The locations of the buildings are representative for relatively soft soil conditions present across the world. The measurement data have first been analyzed in order to identify the first natural frequency of the buildings and the corresponding effective viscous damping ratio. An important result of this analysis is that the effective damp-  
445 ing ratio turned out to be constant in the studied range of building velocities. This means that the damping ratio identified in the course of wind-induced vibrations shows to be independent of the structural velocity. This distinguishes the case of wind-induced vibrations of high-rise buildings (SLS) from the case of earthquake excitation (ULS), in which the level of vibrations enables significant  
450 contribution of nonlinear damping mechanisms to the overall damping. In accordance with the identified velocity-independent damping, linear models have been employed in this study. The Jeary's empirical damping predictor has been used to parametrize the linear viscous damping in the building. This has been done under the assumption that the Wolf's model for embedded foundations is  
455 applicable for description of the effective stiffness and damping of the founda-

tion. The latter model is rather simplistic, but is deemed to be applicable in the low frequency range the first natural frequency of the high-rise buildings belongs in. In the process of parametrization of the model, it has been found that in order to match the measured first natural frequency, the shear wave speed  
460 ( $V_{soil}$ ) of the soil stratum should correspond to rather soft soils with the value being in the range of 100-130 m/s. Using the identified stiffness parameters, the effective viscous damping ratios in the structure and in the foundation have been determined using the 3 degrees-of-freedom model. It has been found that for all admissible parameters of the model, the foundation damping is never lower than  
465 50% of the overall damping. This key result of this paper was critically checked by using the beam model of the building, which differs from the discrete model in the way the structural damping is distributed along the building height. It has been confirmed that for all admissible values of the structural and foundation damping values, the contribution of the latter is always dominant. Based  
470 on the analysis carried out in this paper, it is concluded that the contribution of the foundation damping to the overall damping experienced by a high-rise building on a relatively soft soil is significant indeed and should be accounted for in the design of such buildings.

## References

- 475 [1] J. A. Blume, R. W. Binder, Periods of a modern multi-story office building during construction, Proceedings of the Second World Conference on Earthquake Engineering vol. II (1960) 1195 – 1205.
- [2] H. Ishizaki, N. Hatakeyama, Experimental and numerical studies on vibrations of buildings, Proceedings of the Second World Conference on Earth-  
480 quake Engineering vol. II (1960) 1263–1284.
- [3] D. Hudson, A comparison of theoretical and experimental determinations of building response to earthquakes, Proceedings of the Second World Conference on Earthquake Engineering vol. II (1960) 1105–1119.

- 485 [4] I. Funahashi, K. Kinoshita, H. Aoyama, Vibration tests and test to failure  
of a 7 stories building survived a severe earthquake, Proceedings of the  
Fourth World Conference on Earthquake Engineering vol. I (1969) 26–43.
- [5] G. Hart, M. Lew, R. Di Julio, High-rise building response: Damping and  
period non-linearities, Proceedings of the Fifth World Conference on Earth-  
quake Engineering vol. II (1974) 1440–1444.
- 490 [6] G. Hart, R. Vasudevan, Earthquake design of buildings: damping, Journal  
of the Structural Division ASCE 101 (1975) 11–30.
- [7] J. Collins, J. Young, L. Kiefling, Methods and applications of system iden-  
tification in shock and vibration, Tech. Rep. 73A20429, NASA (1972).
- [8] P. Ibanez, R. Shanman, Identification of dynamic structural models from  
495 experimental data, Proceedings of the Fifth World Conference on Earth-  
quake Engineering vol. I (1974) 290–293.
- [9] H. Kobayashi, Dynamic properties of buildings decided by measurement of  
vibration during earthquake, Proceedings of the Second World Conference  
on Earthquake Engineering vol. II (1960) 1121–1136.
- 500 [10] A. G. Davenport, P. Hill-Carroll, Damping in tall buildings: its variability  
and treatment in design, Proceedings of ASCE Spring Convention (1986)  
42–57.
- [11] A. P. Jeary, Damping in tall buildings—a mechanism and a predictor,  
Earthquake Engineering & Structural Dynamics 14 (5) (1986) 733–750.
- 505 [12] J. Fang, A. Jeary, Q. Li, C. Wong, Random damping in buildings and  
its AR model, Journal of Wind Engineering and Industrial Aerodynamics  
79 (1–2) (1999) 159 – 167.
- [13] S. Lagomarsino, Forecast models for damping and vibration periods of  
buildings, Journal of Wind Engineering and Industrial Aerodynamics  
510 48 (2–3) (1993) 221 – 239.

- [14] N. Satake, K. Suda, T. Arakawa, A. Sasaki, Y. Tamura, Damping evaluation using full-scale data of buildings in japan, *Journal of Structural Engineering* 129 (4) (2003) 470–477.
- [15] R. Emmanuel, R. Aquino, Y. Tamura, On stick–slip phenomenon as primary mechanism behind structural damping in wind-resistant design applications, *Journal of Wind Engineering and Industrial Aerodynamics* 115 (2013) 121 – 136.
- [16] R. Emmanuel, R. Aquino, Y. Tamura, Framework for structural damping predictor models based on stick-slip mechanism for use in wind-resistant design of buildings, *Journal of Wind Engineering and Industrial Aerodynamics* 117 (2013) 25 – 37.
- [17] I. Venanzi, D. Salciarini, C. Tamagnini, The effect of soil–foundation–structure interaction on the wind-induced response of tall buildings, *Engineering Structures* 79 (2014) 117–130.
- [18] J. Avilés, L. E. Pérez-Rocha, Effects of foundation embedment during building–soil interaction, *Earthquake Engineering & Structural Dynamics* 27 (12) (1998) 1523–1540.
- [19] A. S. Veletsos, J. W. Meek, Dynamic behaviour of building-foundation systems, *Earthquake Engineering & Structural Dynamics* 3 (2) (1974) 121–138.
- [20] G. Mylonakis, S. Nikolaou, G. Gazetas, Footings under seismic loading: Analysis and design issues with emphasis on bridge foundations, *Soil Dynamics and Earthquake Engineering* 26 (9) (2006) 824 – 853.
- [21] N. Makris, G. Gazetas, Dynamic pile-soil-pile interaction. part ii: Lateral and seismic response, *Earthquake Engineering & Structural Dynamics* 21 (2) (1992) 145–162.

- [22] M. Novak, L. E. Hifnawy, Effect of soil-structure interaction on damping of structures, *Earthquake Engineering & Structural Dynamics* 11 (5) (1983) 595–621.
- 540 [23] K. Nakagawa, M. Takeuchi, Vibrational characteristics of buildings, part i. Vibrational characteristics of actual buildings determined by actual tests, *Proceedings of the Second Conference on Earthquake Engineering* vol. II (1960) 961–982.
- [24] T. Natio, N. Nasu, M. Takeuchi, G. Kubota, Y. Takana, M. Hara, Vi-  
545 brational characteristics of buildings, part ii. Vibrational charactersitics of reinforced contrecte buildings existing in japan, *Proceedings of the Second World Conference on Earthquake Engineering* vol. II (1960) 982–991.
- [25] J. Wolf, *Foundation vibration analysis using simple physical models*, Prentice Hall, 1995.
- 550 [26] E. Simiu, R. H. Sacanlan, *Wind effects on structures*, John Wiley and sons, 1985.
- [27] H. Marukawa, N. Kato, K. Fujii, Y. Tamura, Experimental evaluation of aerodynamic damping of tall buildings, *Journal of Wind Engineering and Industrial Aerodynamics* 59 (2-3) (1996) 177 – 190.
- 555 [28] X. Chen, Estimation of stochastic crosswind response of wind-excited tall buildings with nonlinear aerodynamic damping, *Engineering Structures* 56 (2013) 766 – 778.
- [29] H. Van Koten, *Deming van bouwconstructies*, Tech. Rep. CUR (1977).
- [30] J. He, Z.-F. Fu, *Modal analysis*, Butterworth Heinemann, Oxford, 2004.